

A codimension-two free boundary problem for the equilibrium shapes of a small three-dimensional island in an epitaxially strained solid film

L. L. SHANAHAN AND B. J. SPENCER[†]

*Department of Mathematics, State University of New York at Buffalo, Buffalo,
NY 14260-2900, USA*

[Received 7 February 2000 and in revised form 15 October 2001]

We determine the equilibrium morphology of a strained solid film for the case where it wets the substrate (Stranski–Krastanow growth). Using a continuum elasticity model with isotropic surface energy and equal elastic constants in the film and substrate, we determine an asymptotic solution for the axisymmetric three-dimensional equilibrium shape of a small island, where the height is much less than the width, resulting in a codimension-two free boundary problem. This codimension-two free boundary problem can be reformulated as an integro-differential equation in which the island width appears as an eigenvalue. The solutions to the resulting integro-differential eigenvalue problem consist of a discrete spectrum of island widths and associated morphological modes, which are determined using a rapidly converging Bessel series. The lowest-order mode is energetically preferred and corresponds to the quantum dot morphology. Our predictions of quantum dot width compare favorably with experimental data in the GeSi/Si system. The higher-order modes, while not minimum-energy configurations, are similar to ‘quantum ring’ and ‘quantum molecule’ morphologies observed during the growth of strained films.

Keywords: Free boundary problem; elasticity; epitaxial film

1. Introduction

Strained solid films are an important component in electronic and opto-electronic devices. In many cases, the desirable growth mode of the film is layer by layer, resulting in a planar film. On the other hand, there has been recent interest in quantum dot devices [23], which correspond to the Stranski–Krastanow growth mode. In the Stranski–Krastanow growth mode, the first few monolayers of the film grow layer by layer, forming a ‘wetting layer’, then subsequent growth occurs in the form of mounds or ‘islands’ on top of the wetting layer (Fig. 1). A review of theoretical and experimental results on island formation is presented in [25].

Morphological evolution in strained solid films can be modeled using continuum theory. The surface of the strained film is treated as a free boundary, and changes in the morphology of the film are due to the diffusion of atoms along the surface, which in turn is linked to a stress-dependent chemical potential. Within this framework, it has been shown that an initially planar film is unstable to the formation of surface corrugations [2, 8–13, 17, 29, 30, 36], the so-called stress-driven morphological instability. If the film is sufficiently thick then the valleys of the corrugation develop cusp singularities in finite time [5, 18, 31, 39, 40]. If the film is sufficiently thin, the deepening of the valley can be stopped by the influence of the substrate. For example, in many systems the surface

[†] To whom correspondence should be addressed

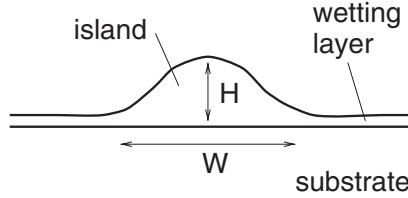


FIG. 1. Schematic illustration of typical island.

energy of the film is lower than that of the substrate, so there is a significant energy penalty for the film to ‘dewet’ the solid surface. Thus, with a strong wetting effect, the substrate surface acts as a barrier for film rupture. Under this constraint, the evolution of the stress-driven instability is towards solid drops (islands) separated by a wetting layer. The island morphology, then, is generated by the strain relief which accompanies the island shape, but also requires the presence of the wetting layer to stabilize the island edges.

Mathematical models for the wetting layer have been investigated in recent years. In general, the details of wetting depend on the atomistic physics of films of a few monolayers thickness (see, for example, [38]). Since the atomistic calculations are difficult (particularly with nonplanar, free boundary geometries) there has been interest in developing robust continuum models for the physics of wetting that enable one to predict the island shape. One idea has been the use of transition layer models, in which the sharp variation in material properties across the film/substrate interface is modeled by a smooth transition over a thin transition layer [6, 19, 41, 42]. Another approach has been to model the wetting layer as being infinitesimally thin, with the wetting energy being much larger than the energetics associated with island formation [32–34]. In this model, the monolayer of the film adjacent to the substrate is in effect ‘glued’ to the substrate. This constraint results in a piecewise boundary condition for the free boundary: the film surface is either $h = 0$ (for the wetting layer), or satisfies a condition of constant chemical potential on the island surface. In this piecewise free boundary description, the island width is to be determined as part of the solution.

Recently, asymptotic results which describe the relationship between the transition layer models and the glued wetting layer model have been presented [35]. It was shown that any transition layer model which has algebraic decay reduces to the glued wetting layer model in the limit of small transition layer thickness. Thus, the results of this analysis suggest that the details of the transition layer model are not important to determining the macroscopic island shape. In view of the correlation between the transition layer models and the glued wetting layer model, we use the glued wetting layer model as the ‘generic’ zero-parameter model for the wetting layer.

It is generally appreciated that islands form because of elastic relaxation: a fixed volume of material has a lower total energy as an island than as a planar film. Of the work on the free boundary problem, there have been asymptotic and numerical solutions for the case of a two-dimensional (2D) ridge [6, 19, 32–35], and recently there have also been calculations of the island shape in three dimensions (3D) using a finite element method with a thick film/substrate transition region [41, 42]. While the 3D calculations hold promise for simulating time-dependent dynamics of well-developed islands, our aim here is to derive some fairly simple asymptotic results that enable one to describe the shape of a small 3D island without extensive computation.

Our analysis is based on the approach used in [32] to describe the shape of a small island ridge. In this work, the solution to the free boundary problem for the island surface was found using an

asymptotic expansion in the aspect ratio of the island (height/width). The resulting problem becomes a codimension-two free boundary problem [15] which consists of a mixed boundary value problem for the half-plane where the location of the points at which the boundary condition changes type are to be determined as part of the solution. At leading order, the island shape was determined as a solution to an integro-differential eigenvalue problem. Here, we employ the same approach to determine the shape of an axisymmetric island.

The codimension-two free boundary problem for the island shape consists of an integro-differential equation with prescribed boundary conditions at the island edges, the position of which is to be determined. The island width plays the role of an eigenvalue, and we find a discrete spectrum of island widths and associated morphological modes which can be indexed by the number of ridges on the island surface, m .

The lowest-order mode $m = 1$ corresponds to the quantum dot morphology and is the most energetically favorable mode. The width is the minimum width of the island modes, and is almost a factor of two larger than the width of a small island ridge, a result that is consistent with the energetics of 3D versus 2D small-amplitude surface undulations. We compare our predictions of the island width directly to experimental data and find that our theory is consistent with observations of small islands in the GeSi/Si system.

Other low-order modes are less energetically favorable than the quantum dot mode, but may be physically relevant as metastable states. In particular, the modes $m = 2$ and $m = 3$ are similar to quantum ring and quantum molecule morphologies. We suggest generalizations of our axisymmetric solutions to non-axisymmetric, annular solutions which may permit quantitative description of the quantum ring and quantum molecule morphologies and energetics.

The remainder of the paper is organized as follows. In Section 2 we construct the mathematical model and nondimensionalize the system. In Section 3 we seek solutions as an asymptotic expansion in the island aspect ratio and obtain the integro-differential eigenvalue problem for the island shape, which we solve using a Bessel series. In Section 4 we compare the results for our quantum dot solution to the 2D theory and to experiments, and describe the relevance of our other solutions to quantum rings and quantum molecules. Section 5 summarizes our findings.

2. Mathematical model

2.1 Variational problem for the island shape

We model the Stranski–Krastanow morphology in a 3D, isotropic, epitaxially strained system, and describe the shape of an axisymmetric, isolated island. As described in Section 1, the formation of islands requires a model for the wetting interaction of the film and substrate. We use the glued wetting layer model in which a wetting layer of negligible thickness covers the substrate, and such that the energy required to remove the wetting layer from the substrate is large relative to the energies involved in the formation of the islands. Thus, in the context of our continuum model, the wetting layer is a layer of the film of vanishing thickness which is in effect glued to the substrate [32].

We describe the island shape in cylindrical coordinates with radial symmetry, $z = h(r)$. The wetting model then dictates that $h(r) \geq 0$. For an isolated island of finite dimensions the film thickness vanishes outside some radius R describing the island size, and

$$\begin{cases} h(r) \geq 0 & \text{for } 0 < r < R \\ h(r) = 0 & \text{for } r \geq R. \end{cases} \quad (2.1)$$

The equilibrium island shape can be described by the solution to a variational problem for minimizing the energy of the system subject to the constraint of constant volume of the film and the wetting constraint. The energy consists of two contributions, $E = E_\gamma + E_S$ where

$$E_\gamma = \int_{\mathcal{S}} \gamma \, d\mathcal{S} \quad (2.2)$$

is the total surface energy obtained by integrating the surface free energy density γ over the surface of the film \mathcal{S} , and where

$$E_S = \int_{\mathcal{V}} S(u, h) \, d\mathcal{V} \quad (2.3)$$

is the total strain energy of the system obtained by integrating the linear elasticity strain energy density $S(u, h)$ over the volume of the film and substrate. Here $S(u, h)$ denotes the dependence of the strain energy on the displacement field u and the shape of the domain h . Finally, for radial symmetry the volume constraint takes the form

$$V = 2\pi \int_0^R h(r) r \, dr, \quad (2.4)$$

where V is the prescribed volume of the island.

Minimizing E with respect to variations in the shape h and variations in the displacement u for prescribed V and $h \geq 0$ results in a variational inequality for h coupled to the linear elasticity equations. The volume constraint enters with a Lagrange multiplier μ (the chemical potential). The contact angle condition arising from the variational calculation is that $h'(r) = 0$ at the island edges because the surface energy of the island and the surface energy of the wetting layer are the same. This classical Young angle is not modified by the presence of elastic strain, as has been shown from the local analysis of possible singularities for arbitrary contact angle [37]. The equation for the shape of the island is then determined by the piecewise boundary condition

$$\begin{cases} h'(r) = 0 & \text{at } r = 0 \text{ (by symmetry)} \\ \mu = \gamma\kappa(h) + S(u, h) & \text{for } h(r) > 0 \text{ (on the island)} \\ h'(r) = 0 & \text{at the island edge} \\ h(r) = 0 & \text{otherwise (on the wetting layer)} \end{cases} \quad (2.5)$$

where κ is the local curvature of the film surface, and $S(u, h)$ is the strain energy density evaluated at the surface of the film. Equilibrium island shapes correspond to finding solutions $h(r)$ which satisfy (2.5) for constant chemical potential μ (the value of which is to be determined). As written, (2.5) might permit solutions consisting of concentric annular island ‘rings’ separated by wetting layers of zero thickness. Our aim in this paper is to describe the shape of a single island as is commonly observed in experiments and for which $h(r) > 0$ on $0 < r < R$. To this end, we assume that $h(r) > 0$ for $0 < r < R$ to rule out the possibility of a ‘ring’ structure (in Section 4 we suggest extending this work to permit the description of ring-like solutions). The equation for the island shape is then

$$\begin{cases} h'(r) = 0 & \text{at } r = 0 \\ \mu = \gamma\kappa(h) + S(u, h) & \text{for } 0 < r < R \text{ (on the island)} \\ h'(r) = 0 & \text{at } r = R \\ h(r) = 0 & \text{for } r \geq R. \end{cases} \quad (2.6)$$

Note that the location of the island edge R and the chemical potential μ are to be determined.

The minimization of the energy with respect to the displacement yields the usual equations of linear elasticity, with a jump condition on the strains at the film/substrate interface to account for the misfit strain due to the difference in lattice parameters in the film and substrate. For lattice parameters of the film a_F and the substrate a_S , the biaxial misfit strain is $\epsilon_m = (a_S - a_F)/a_F$ in the film at the film/substrate interface. For our islands with assumed radial symmetry, the linear elasticity problem for mechanical equilibrium in the film/substrate system is given by the following system of equations. Defining σ^F and σ^S as the stress tensors in the film and substrate, respectively, mechanical equilibrium in the solid requires

$$\nabla \cdot \sigma^F = 0 \quad \text{in the film } (0 < z < h(r)) \quad (2.7)$$

and

$$\nabla \cdot \sigma^S = 0 \quad \text{in the substrate } (z < 0), \quad (2.8)$$

subject to the Beltrami–Michell compatibility conditions. The boundary conditions for the elasticity problem are the following. First, the film surface is traction free,

$$\sigma^F \cdot \mathbf{n} = 0 \quad \text{on } z = h(r) \quad (2.9)$$

where \mathbf{n} is the outward unit normal to the film surface. Second, there is a force balance at the film/substrate interface,

$$\sigma^F \cdot \hat{\mathbf{z}} = \sigma^S \cdot \hat{\mathbf{z}} \quad \text{on } z = 0 \quad (2.10)$$

where $\hat{\mathbf{z}}$ is the unit normal in the z direction. Third, the misfit strain generated by the difference in lattice parameters generates a jump in the lateral components of the strain tensor \mathbf{E} across the film/substrate interface,

$$\begin{aligned} E_{rr}^F &= E_{rr}^S + \epsilon_m & \text{on } z = 0 \\ E_{\theta\theta}^F &= E_{\theta\theta}^S + \epsilon_m & \text{on } z = 0 \\ E_{rz}^F &= E_{rz}^S & \text{on } z = 0 \\ E_{\theta z}^F &= E_{\theta z}^S & \text{on } z = 0 \end{aligned} \quad (2.11)$$

where the subscripts denote the components of the strain tensor in cylindrical coordinates. The last boundary condition is that the stresses in the substrate decay to zero far away from the island,

$$\sigma^S \rightarrow 0 \quad \text{as } z \rightarrow -\infty \text{ and as } r \rightarrow \infty. \quad (2.12)$$

Finally, in each of the film and substrate we use isotropic linear elasticity to relate stress to strain,

$$\sigma = \frac{E}{1 + \nu} \left[\mathbf{E} + \frac{\nu}{1 - 2\nu} \text{Tr}(\mathbf{E}) \mathbf{I} \right], \quad (2.13)$$

where E is Young's modulus, ν is Poisson's ratio, $\text{Tr}(\mathbf{E})$ is the trace of the strain tensor, and \mathbf{I} is the identity tensor. Equations (2.4) and (2.6)–(2.13) define the free boundary problem for

the equilibrium shape of an isolated, axisymmetric non-annular strained island with prescribed volume V .

It can be shown that the above equations can also be derived by using an alternative to the wetting constraint $h \geq 0$. If one considers a class of wetting layer models that are based on a smooth transition in material properties across the film/substrate interface, then, in the limit that the transition layer thickness approaches zero, one recovers the 2D version of the equations above [35]. Viewed in this way, the free boundary equation (2.6) can be interpreted as the condition of constant chemical potential μ over the entire film surface: over the island surface the strain energy and surface energy balance to give the island shape, and in the wetting layer the strain energy and wetting energies balance. Further, the contact angle condition $h' = 0$ at the island edge also results naturally from matching solutions for the wetting layer and the island.

2.2 Nondimensionalization

We nondimensionalize the model by using the misfit stress and misfit strain in a planar film as characteristic scales for the stress and strain fields. The planar film has a characteristic biaxial stress tensor σ_0 with magnitude $\sigma_0 = \epsilon_m E / (1 - \nu)$, and a corresponding strain energy density $S_0 = \epsilon_m^2 E / (1 - \nu)$. We use a characteristic length of $l = \gamma / S_0$.

In most systems the film and the substrate have similar elastic properties, so to greatly simplify the elasticity problem we assume that the film and substrate have the same elastic constants. In this case the elasticity problem with the jump condition on the strains at the film/substrate interface and decay of the stress in the substrate as $z \rightarrow -\infty$ is equivalent to a problem where one imposes the misfit stress at $z \rightarrow -\infty$ with continuity of strain at the film/substrate interface. We thus define the scaled stress field \mathbf{T} as given by $\mathbf{T} = \boldsymbol{\sigma}^F / \sigma_0$ in the film and $\mathbf{T} = (\boldsymbol{\sigma}^S + \boldsymbol{\sigma}_0) / \sigma_0$ in the substrate, where the role of $\boldsymbol{\sigma}_0$ in $\boldsymbol{\sigma}^S$ is to eliminate ϵ_m from the film/substrate boundary condition. In this case the conditions for \mathbf{T} on the film/substrate interface reduce to the usual continuity conditions that apply to any interior plane of a solid, and the film/substrate interface serves only as a dividing surface that distinguishes film from substrate. The linear elasticity problem becomes

$$\nabla \cdot \mathbf{T} = 0 \quad \text{in } z < h(r) \quad (2.14)$$

$$\mathbf{T} \cdot \mathbf{n} = 0 \quad \text{on } z = h(r) \quad (2.15)$$

and

$$\mathbf{T} \rightarrow \begin{bmatrix} 1 & 0 & 0 \\ 0 & 1 & 0 \\ 0 & 0 & 0 \end{bmatrix} \quad \text{as } z \rightarrow -\infty \text{ and as } r \rightarrow \infty \quad (2.16)$$

where

$$\mathbf{T} = \begin{bmatrix} \sigma_{rr} & \tau_{r\theta} & \tau_{rz} \\ \tau_{r\theta} & \sigma_{\theta\theta} & \tau_{\theta z} \\ \tau_{rz} & \tau_{\theta z} & \sigma_{zz} \end{bmatrix}. \quad (2.17)$$

The scaled conditions on the free boundary are given by

$$\begin{cases} h'(r) = 0 & \text{at } r = 0 \\ \mu = \kappa(h) + S(h) & \text{for } 0 \leq r < R \\ h'(r) = 0 & \text{at } r = R \\ h(r) = 0 & \text{for } r \geq R, \end{cases} \quad (2.18)$$

where

$$\kappa(h) = -\frac{1}{r} \frac{d}{dr} \left(r \frac{dh}{dr} / \sqrt{1 + (dh/dr)^2} \right), \quad (2.19)$$

and

$$S(h) = \frac{1}{2(1-\nu)} [(1+\nu)(\sigma_{rr}^2 + \sigma_{\theta\theta}^2 + \sigma_{zz}^2) - \nu\sigma_{kk}^2 + 2(1+\nu)\tau_{rz}^2], \quad (2.20)$$

where ν is Poisson's ratio and $\sigma_{kk} = \text{Tr}(\mathbf{T})$. Finally, the volume constraint in nondimensional form is

$$V = 2\pi \int_0^R h(r)r \, dr. \quad (2.21)$$

All variables are now non-dimensional with respect to the appropriate length or energy scale. The film/substrate interface has been eliminated from the elasticity problem by the assumptions of a planar interface and equal elastic constants in film and substrate. The resulting elasticity problem is equivalent to a biaxially stressed, semi-infinite isotropic solid.

3. Asymptotic solutions for thin islands

3.1 Thin island scalings

We now describe an island where the height H is assumed to be much smaller than the island width $W \equiv 2R$, corresponding to a small 'flat' island (see Fig. 1). We choose a characteristic island height H_c such that $H_c = \epsilon$. The scaled island shape is then given by $\tilde{h}(r) = h(r)/\epsilon$, with the nondimensional volume constraint

$$V = 2\pi\epsilon \int_0^R \tilde{h}(r)r \, dr. \quad (3.1)$$

In what follows we show that for $H_c = \epsilon$, the island half-width R remains $O(1)$. Thus, the island volume has the same scaling as H_c , with $V = O(\epsilon)$. Rather than defining H_c as the precise height of the island H , we instead choose to define $\epsilon = V$. In this case the volume constraint on $\tilde{h}(r)$ becomes

$$2\pi \int_0^R \tilde{h}(r)r \, dr = 1, \quad (3.2)$$

and the island height H is $O(\epsilon)$. The scaled boundary condition for the thin island is then

$$\begin{cases} \tilde{h}'(0) = 0 \\ \mu = \epsilon\tilde{\kappa} + S & \text{for } 0 \leq r < R \\ \tilde{h}'(R) = 0 \\ \tilde{h}(r) = 0 & \text{for } r \geq R, \end{cases} \quad (3.3)$$

where $\kappa = \epsilon\tilde{\kappa}$, and the scaled axisymmetric elasticity problem is

$$-\epsilon \frac{d\tilde{h}}{dr} \sigma_{rr} + \tau_{rz} = 0 \quad \text{on } z = \epsilon\tilde{h}(r) \quad (3.4)$$

$$-\epsilon \frac{d\tilde{h}}{dr} \tau_{rz} + \sigma_{zz} = 0 \quad \text{on } z = \epsilon\tilde{h}(r) \quad (3.5)$$

with

$$\frac{\partial \sigma_{rr}}{\partial r} + \frac{\partial \tau_{rz}}{\partial z} + \frac{\sigma_{rr} - \sigma_{\theta\theta}}{r} = 0 \quad \text{in } z < \epsilon\tilde{h}(r) \quad (3.6)$$

$$\frac{\partial \tau_{rz}}{\partial r} + \frac{\partial \sigma_{zz}}{\partial z} + \frac{\tau_{rz}}{r} = 0 \quad \text{in } z < \epsilon\tilde{h}(r) \quad (3.7)$$

and with

$$\mathbf{T} \rightarrow \begin{bmatrix} 1 & 0 & 0 \\ 0 & 1 & 0 \\ 0 & 0 & 0 \end{bmatrix} \quad \text{as } z \rightarrow -\infty \text{ and as } r \rightarrow \infty. \quad (3.8)$$

3.2 Thin island expansion

We look for an asymptotic solution to the free boundary problem in powers of ϵ of the form

$$\tilde{h}(r) = \tilde{h}_0(r) + \epsilon \tilde{h}_1(r) + \dots \quad (3.9)$$

$$R = R_0 + \epsilon R_1 + \dots \quad (3.10)$$

$$\mathbf{T}(r, z) = \mathbf{T}^{(0)} + \epsilon \mathbf{T}^{(1)} + \dots \quad (3.11)$$

$$\mu = \mu_0 + \epsilon \mu_1 + \dots \quad (3.12)$$

$$S(r, \epsilon\tilde{h}(r)) = S_0 + \epsilon S_1 + \dots \quad (3.13)$$

$$\tilde{\kappa} = \tilde{\kappa}_0 + \epsilon \tilde{\kappa}_1 + \dots \quad (3.14)$$

We substitute the expansions into the governing equations, drop tildes and collect like terms by order in ϵ .

3.3 $O(1)$ solution

At $O(1)$ the elasticity problem corresponds to the biaxially stressed half-space,

$$\tau_{rz}^{(0)} = 0 \quad \text{on } z = 0 \quad (3.15)$$

$$\sigma_{zz}^{(0)} = 0 \quad \text{on } z = 0 \quad (3.16)$$

with

$$\nabla \cdot \mathbf{T}^{(0)} = 0 \quad \text{in } z < 0 \quad (3.17)$$

and

$$\mathbf{T}^{(0)} \rightarrow \begin{bmatrix} 1 & 0 & 0 \\ 0 & 1 & 0 \\ 0 & 0 & 0 \end{bmatrix} \quad \text{as } z \rightarrow -\infty \text{ and as } r \rightarrow \infty. \quad (3.18)$$

The only contribution from the free boundary condition is the chemical potential condition

$$\mu_0 = S_0 \quad \text{for } 0 \leq r < R_0. \quad (3.19)$$

Thus, with $\mathbf{T}^{(0)}$ corresponding to uniform biaxial stress in the far field, we have $\mu_0 = S_0 = 1$. The leading order shape h_0 is undetermined at this order.

3.4 $O(\epsilon)$ solution

At $O(\epsilon)$ we obtain the elasticity problem for a half-space,

$$\frac{\partial \sigma_{rr}^{(1)}}{\partial r} + \frac{\partial \tau_{rz}^{(1)}}{\partial z} + \frac{\sigma_{rr}^{(1)} - \sigma_{\theta\theta}^{(1)}}{r} = 0 \quad \text{in } z < 0 \quad (3.20)$$

$$\frac{\partial \tau_{rz}^{(1)}}{\partial r} + \frac{\partial \sigma_{zz}^{(1)}}{\partial z} + \frac{\tau_{rz}^{(1)}}{r} = 0 \quad \text{in } z < 0 \quad (3.21)$$

with the boundary conditions

$$\tau_{rz}^{(1)} = \frac{dh_0}{dr} \quad \text{on } z = 0 \quad (3.22)$$

$$\sigma_{zz}^{(1)} = 0 \quad \text{on } z = 0 \quad (3.23)$$

$$\mathbf{T}^{(1)} \rightarrow 0 \quad \text{as } z \rightarrow -\infty \text{ and as } r \rightarrow \infty. \quad (3.24)$$

Using the boundary condition (3.23) to eliminate $\sigma_{zz}^{(1)}$ from the elastic energy density S_1 , the free boundary condition is

$$h_0'(0) = 0 \quad (3.25)$$

$$\mu_1 = (\sigma_{rr}^{(1)} + \sigma_{\theta\theta}^{(1)}) - \frac{1}{r} \frac{d}{dr} \left(r \frac{dh_0}{dr} \right) \quad \text{for } 0 \leq r < R_0 \quad (3.26)$$

$$h_0'(R_0) = 0 \quad (3.27)$$

$$h_0(r) = 0 \quad \text{for } R_0 \leq r < \infty, \quad (3.28)$$

and the volume constraint gives

$$2\pi \int_0^{R_0} h_0(r) r \, dr = 1. \quad (3.29)$$

The goal is to find $h_0(r)$ which satisfies the edge conditions and volume constraint and for which the corresponding stress $\mathbf{T}^{(1)}$ from (3.20)–(3.24) results in (3.26) being satisfied. Note that R_0 and μ_1 are constants to be determined.

The $O(\epsilon)$ problem is thus a codimension-two free boundary problem of the type reviewed by Howison *et al.* [15] where the proximity of the free boundary to a prescribed surface leads to a mixed boundary value problem on a prescribed domain, but with the locations of the points where the boundary condition changes type (R_0 in our case) to be determined as a free boundary. Their review surveyed recent work on such problems involving either Laplace's equation or the biharmonic equation in the half-plane. Our problem involves mechanical equilibrium in an axisymmetric half-space, so we can formulate it as an axisymmetric biharmonic problem (see the Appendix). While the island shape problem is reminiscent of elastic contact problems, here the applied traction in the contact region is a shear stress which depends on the island slope, and the island shape itself is determined by a balance of curvature and elastic strain energy. Thus, it possibly represents a new type of codimension-two problem which involves the biharmonic potential. One feature of codimension-two problems discussed by Howison *et al.* is that it is usually hard to determine the appropriate edge conditions, particularly in the dynamic case. In our case, we are only seeking equilibrium solutions, and the contact angle condition at the island edges (the classical Young angle) is well established from local scaling arguments [37] and asymptotic analysis of a parent problem [35]. Finally, the presence of the additional unknown μ_1 in our case is balanced by the additional volume constraint.

In the Appendix we derive the elasticity solution to (3.20)–(3.24) using Hankel transforms. The stress terms appearing in (3.26) corresponding to the elastic energy density S_1 are related to the island shape by

$$(\sigma_{rr}^{(1)} + \sigma_{\theta\theta}^{(1)}) = 2(1 + \nu) \int_0^\infty \xi \left[\int_0^{R_0} \hat{r} \frac{dh_0}{d\hat{r}} J_1(\xi \hat{r}) d\hat{r} \right] J_0(\xi r) d\xi. \quad (3.30)$$

Substituting this expression into (3.26) we obtain the integro-differential equation for the island shape

$$\mu_1 = 2(1 + \nu) \int_0^\infty \xi \left[\int_0^{R_0} \hat{r} \frac{dh_0}{d\hat{r}} J_1(\xi \hat{r}) d\hat{r} \right] J_0(\xi r) d\xi - \frac{1}{r} \frac{d}{dr} \left(r \frac{dh_0}{dr} \right) \quad 0 \leq r < R_0, \quad (3.31)$$

which is augmented by the volume constraint (3.29) and the boundary conditions

$$h'(0) = 0 \quad (3.32)$$

$$h'(R_0) = 0 \quad (3.33)$$

$$h(R_0) = 0. \quad (3.34)$$

The values of the island radius R_0 and the chemical potential μ_1 are to be determined. The above integro-differential system can be viewed as an obstacle problem with a nonlocal operator.

To analyze (3.31) we rescale lengths by

$$s = r/R_0 \quad (3.35)$$

and

$$H(s) = h_0(r)/R_0 \quad (3.36)$$

to fix the domain of the equation as $0 \leq s < 1$. Also, the presence of Poisson's ratio ν in (3.31) can be absorbed by defining

$$\hat{\mu} = \frac{\mu_1}{1 + \nu} \quad (3.37)$$

and

$$\hat{R} = R_0(1 + \nu). \quad (3.38)$$

With these rescalings and $\xi \rightarrow \xi/R_0$, the integro-differential equation becomes

$$\hat{\mu} = 2 \int_0^\infty \xi \left[\int_0^1 \hat{s} \frac{dH}{d\hat{s}} J_1(\xi \hat{s}) d\hat{s} \right] J_0(\xi s) d\xi - \frac{1}{\hat{R}} \frac{1}{s} \frac{d}{ds} \left(s \frac{dH}{ds} \right) \quad 0 \leq s < 1, \quad (3.39)$$

with the boundary conditions

$$H'(0) = 0 \quad (3.40)$$

$$H'(1) = 0 \quad (3.41)$$

$$H(1) = 0 \quad (3.42)$$

and the volume constraint

$$2\pi \left(\frac{\hat{R}}{1 + \nu} \right)^3 \int_0^1 H(s) s ds = 1 \quad (3.43)$$

which now contains the dependence on ν . In our solutions to (3.39), \hat{R} is determined as a necessary condition for solutions to exist and plays the role of an eigenvalue. The unknown constant $\hat{\mu}$ is determined as a property of those solutions.

The role of \hat{W} and $\hat{\mu}$ in the solutions can be illustrated more clearly by introducing the alternate scaling $H(s) = \hat{\mu} \hat{H}(s)$ which transfers $\hat{\mu}$ from the integral equation to the volume constraint, determining it in terms of $\hat{H}(r)$:

$$\hat{\mu} = \left(2\pi \hat{R}_0^3 \int_0^1 \hat{H}(s) s ds \right)^{-1}. \quad (3.44)$$

Upon applying $\int_0^s (\cdot) s ds$ to the integral equation for $\hat{H}(s)$ we obtain a Fredholm integral equation of the second kind for $d\hat{H}/ds$,

$$\frac{s}{2} = 2 \int_0^1 \hat{s} \frac{d\hat{H}}{d\hat{s}} P(s, \hat{s}) d\hat{s} - \frac{1}{\hat{R}} \frac{d\hat{H}}{ds} \quad (3.45)$$

where

$$P(s, \hat{s}) = \int_0^\infty J_1(\xi s) J_1(\xi \hat{s}) d\xi = \frac{2}{\pi s_*} \left[K \left(\frac{s_*}{s_\dagger} \right) - E \left(\frac{s_*}{s_\dagger} \right) \right], \quad (3.46)$$

and where K , E , are the complete elliptic integrals of the first and second kind, respectively, $s_* = \min(s, \hat{s})$ and $s_\dagger = \max(s, \hat{s})$. Of the solutions $\hat{H}(s; \hat{R})$ to (3.45), we seek those for which

$\hat{H}'(0) = \hat{H}'(1) = 0$. Thus \hat{R} plays the role of an eigenvalue, but it is not the eigenvalue of the integral operator. Our numerical results in the next section show that there is a discrete spectrum of \hat{R} for which solutions to the integral equation also satisfy the boundary conditions. Once $\hat{H}'(r)$ is known from the integral equation, $\hat{H}(r)$ can be determined from integration using $\hat{H}(1) = 0$ and then $\hat{\mu}$ can be determined from the volume constraint above. While (3.45) is an alternative form for (3.39) which illustrates the role of \hat{R} and $\hat{\mu}$, we develop our numerical solutions from the unrescaled version (3.39).

3.5 Bessel series solutions

We seek numerical solutions to the integro-differential equation (3.39) with boundary conditions (3.40)–(3.42) and volume constraint (3.43). We pose a Bessel series expansion for $H(s)$ that satisfies the three boundary conditions (3.40)–(3.42):

$$H(s) = \begin{cases} a_0 + \sum_{k=1}^{\infty} a_k J_0(\mathcal{Z}_k s) & \text{for } 0 \leq s < 1 \text{ (on the island)} \\ 0 & \text{otherwise (on the wetting layer)} \end{cases} \quad (3.47)$$

where (3.40) and (3.41) are satisfied by choosing \mathcal{Z}_k ($k = 1, 2, \dots$) to be the zeros of J_1 , and (3.42) is satisfied by requiring

$$a_0 = - \sum_{k=1}^{\infty} a_k J_0(\mathcal{Z}_k). \quad (3.48)$$

Using the relation $J_0'(x) = -J_1(x)$ we find

$$\frac{dH}{ds} = - \sum_{k=1}^{\infty} a_k \mathcal{Z}_k J_1(\mathcal{Z}_k s). \quad (3.49)$$

We substitute the series into the integro-differential equation (3.39) and obtain

$$\begin{aligned} \hat{\mu} = & -2 \int_0^{\infty} \xi \left[\int_0^1 \hat{s} \sum_{k=1}^{\infty} a_k \mathcal{Z}_k J_1(\mathcal{Z}_k \hat{s}) J_1(\xi \hat{s}) d\hat{s} \right] J_0(\xi s) d\xi \\ & + \frac{1}{\hat{R}} \frac{1}{s} \frac{d}{ds} \left(s \sum_{k=1}^{\infty} a_k \mathcal{Z}_k J_1(\mathcal{Z}_k s) \right) \quad \text{for } 0 \leq s < 1. \end{aligned} \quad (3.50)$$

The operator $\int_0^1 (\cdot) s J_0(\mathcal{Z}_j s) ds$ is applied to each term of (3.50) to obtain a linear system of equations for the coefficients a_k . We first consider the cases for $j = 1, 2, \dots$ (the case of $j = 0$ will be considered separately later). Applying the operator to the left-hand side of (3.50) we have

$$\int_0^1 s \hat{\mu} J_0(\mathcal{Z}_j s) ds = \frac{\hat{\mu} J_1(\mathcal{Z}_j)}{\mathcal{Z}_j} = 0 \quad (3.51)$$

since $J_1(\mathcal{Z}_j) = 0$. We apply the operator to the first term on the right-hand side of the integro-differential equation (3.50) and rewrite the result to obtain

$$-2 \sum_{k=1}^{\infty} a_k \mathcal{Z}_k \int_0^1 s J_0(\mathcal{Z}_j s) \int_0^{\infty} \xi \left[\int_0^1 \hat{s} J_1(\mathcal{Z}_k \hat{s}) J_1(\xi \hat{s}) d\hat{s} \right] J_0(\xi s) d\xi ds. \quad (3.52)$$

The \hat{s} integral can be evaluated analytically. The result is

$$\int_0^1 \hat{s} J_1(\mathcal{Z}_k \hat{s}) J_1(\xi \hat{s}) d\hat{s} = \frac{[\mathcal{Z}_k J_1(\xi) J_1'(\mathcal{Z}_k) - \xi J_1(\mathcal{Z}_k) J_1'(\xi)]}{\xi^2 - \mathcal{Z}_k^2}. \quad (3.53)$$

Using the fact that $J_1(\mathcal{Z}_k) = 0$ and using the recurrence relation $J_n'(x) = J_{n-1}(x) - nJ_n(x)/x$ gives the analytical result to the first integration of

$$-2 \sum_{k=1}^{\infty} a_k \mathcal{Z}_k \int_0^1 s J_0(\mathcal{Z}_j s) \int_0^{\infty} \frac{\xi \mathcal{Z}_k J_1(\xi) J_0(\mathcal{Z}_k)}{(\xi^2 - \mathcal{Z}_k^2)} J_0(\xi s) d\xi ds. \quad (3.54)$$

Interchanging the order of integration and repeating the procedure on the s integral with the relationship $J_0'(x) = -J_1(x)$ gives the integrated term

$$-2 \sum_{k=1}^{\infty} a_k \mathcal{Z}_k^2 J_0(\mathcal{Z}_k) J_0(\mathcal{Z}_j) \int_0^{\infty} \frac{\xi^2 J_1^2(\xi)}{(\xi^2 - \mathcal{Z}_k^2)(\xi^2 - \mathcal{Z}_j^2)} d\xi. \quad (3.55)$$

Note that if $\xi = \mathcal{Z}_j$ or $\xi = \mathcal{Z}_k$ then $J_1^2(\xi) = 0$, so the apparent singularities in (3.55) are removable and the integral is well behaved. Applying the operator to the third term of the integro-differential equation (3.50) gives

$$\frac{1}{\hat{R}} \sum_{k=1}^{\infty} a_k \mathcal{Z}_k \int_0^1 \frac{d}{ds} (s J_1(\mathcal{Z}_k s)) J_0(\mathcal{Z}_j s) ds. \quad (3.56)$$

Using the recurrence relation $\frac{d}{dx} \{x^n J_n(x)\} = x^n J_{n-1}(x)$, (3.56) can be rewritten as

$$\frac{1}{\hat{R}} \sum_{k=1}^{\infty} a_k \mathcal{Z}_k^2 \int_0^1 s J_0(\mathcal{Z}_k s) J_0(\mathcal{Z}_j s) ds. \quad (3.57)$$

Since orthogonality holds for (3.57) even with \mathcal{Z}_k as the zeros of J_1 instead of J_0 , only the $k = j$ term contributes to the sum and the result is

$$\frac{1}{2\hat{R}} a_j \mathcal{Z}_j^2 J_0^2(\mathcal{Z}_j). \quad (3.58)$$

Having applied the operator to all pieces of (3.50), the transformed integro-differential equation is the linear system

$$0 = -2 \sum_{k=1}^{\infty} a_k \mathcal{Z}_k^2 J_0(\mathcal{Z}_k) J_0(\mathcal{Z}_j) Q(\mathcal{Z}_j, \mathcal{Z}_k) + \frac{1}{2\hat{R}} a_j \mathcal{Z}_j^2 J_0^2(\mathcal{Z}_j) \quad j = 1, 2, \dots \quad (3.59)$$

where

$$Q(\mathcal{Z}_j, \mathcal{Z}_k) = \int_0^{\infty} \frac{\xi^2 J_1^2(\xi)}{(\xi^2 - \mathcal{Z}_k^2)(\xi^2 - \mathcal{Z}_j^2)} d\xi. \quad (3.60)$$

Equation (3.59) is a homogeneous linear system for the coefficients a_k which can be written as $\mathbf{M}\mathbf{a} = 0$, where \mathbf{a} is the coefficient vector and the components of the matrix \mathbf{M} are

$$M_{jk} = -2Z_k^2 J_0(Z_k) J_0(Z_j) Q(Z_j, Z_k) + \delta_{jk} \frac{Z_j^2}{2\hat{R}} J_0^2(Z_j) \quad (3.61)$$

with

$$\delta_{jk} = \begin{cases} 1 & \text{if } j = k \\ 0 & \text{if } j \neq k. \end{cases} \quad (3.62)$$

The linear system depends on the island radius \hat{R} through the diagonal terms of \mathbf{M} . In general, the homogeneous linear system has only the trivial solution $\mathbf{a} = 0$. A nontrivial solution requires \mathbf{M} to be singular, which determines the eigenvalue \hat{R} . Note that \hat{R} is not given by the eigenvalues of the matrix \mathbf{M} , but rather corresponds to the weighting of the diagonal term in (3.61) which makes the matrix singular.

The eigenvalue problem (3.59) for the island radius \hat{R} can be converted to the standard matrix eigenvalue problem with a diagonal transformation. We write (3.59) as

$$(-\mathbf{B} + \lambda\mathbf{D})\mathbf{a} = 0 \quad (3.63)$$

where $\lambda = 1/(2\hat{R})$ and \mathbf{D} is the diagonal matrix appearing as the second term in (3.61). Let

$$\mathbf{u} = \mathbf{D}\mathbf{a} \quad (3.64)$$

and define

$$\mathbf{A} = \mathbf{B}\mathbf{D}^{-1} \quad (3.65)$$

where

$$A_{jk} = 2 \frac{J_0(Z_j)}{J_0(Z_k)} Q(Z_j, Z_k) \quad (3.66)$$

to obtain the standard eigenvalue problem

$$\mathbf{A}\mathbf{u} = \lambda\mathbf{u}. \quad (3.67)$$

From the eigensolutions (λ, \mathbf{u}) we find $\hat{R} = 1/2\lambda$ and calculate the coefficients in the expansion from $\mathbf{a} = \mathbf{D}^{-1}\mathbf{u}$ to find

$$a_k = \frac{u_k}{Z_k^2 J_0(Z_k)^2}. \quad (3.68)$$

Once a_k ($k = 1, 2, \dots$) are determined from the eigenvalue problem, a_0 is determined from (3.48).

To implement the volume constraint (3.43) we note that since (3.59) is homogeneous, the solutions \mathbf{a} have an arbitrary multiplicative scale factor c such that $c\mathbf{a}$ is also a solution. The scale factor c is determined from the volume constraint (3.43) to be

$$c = \frac{(1 + \nu)^3}{\pi a_0 \hat{R}^3}. \quad (3.69)$$

Finally, the chemical potential $\hat{\mu}$ is determined by applying the operator $\int_0^1 s(\cdot) ds$ (the $j = 0$ case alluded to previously) to the three terms of (3.50). The first term gives

$$\int_0^1 s \hat{\mu} ds = \frac{\hat{\mu}}{2}. \quad (3.70)$$

The second term gives

$$-2 \sum_{k=1}^{\infty} a_k Z_k \int_0^1 s \int_0^{\infty} \frac{\xi Z_k J_1(\xi) J_0(Z_k)}{\xi^2 - Z_k^2} J_0(\xi s) d\xi ds. \quad (3.71)$$

Interchanging the integrals and using the relation $\int x J_0(x) dx = x J_1(x)$ leads to

$$-2 \sum_{k=1}^{\infty} a_k Z_k^2 J_0(Z_k) \int_0^{\infty} \frac{J_1^2(\xi)}{(\xi^2 - Z_k^2)} d\xi. \quad (3.72)$$

The third term gives

$$\int_0^1 s \left[\frac{-1}{\hat{R}s} \frac{d}{ds} \left(s \frac{dH}{ds} \right) \right] ds = 0, \quad (3.73)$$

where we have used the boundary conditions $H'(1) = 0$ and $H'(0) = 0$ for the island shape. Thus, the chemical potential is

$$\hat{\mu} = -4c \sum_{k=1}^{\infty} a_k Z_k^2 J_0(Z_k) \int_0^{\infty} \frac{J_1^2(\xi)}{(\xi^2 - Z_k^2)} d\xi, \quad (3.74)$$

where, again, the singularity at $\xi = Z_k$ is removable.

3.6 Numerical solutions

We construct an approximate numerical solution for the island shape by truncating the series at N terms, resulting in \mathbf{M} being an $N \times N$ matrix. We solve the matrix eigenvalue problem (3.67) using Maple 6. The integrations in the coefficients of \mathbf{A} are of an oscillatory integrand (call the integrand $q(\xi)$) on an infinite domain, so we have used the asymptotic behavior of the integrand $q(\xi) \sim q_*(\xi)$ for $\xi \gg 1$ to write each integral as $\int_0^{\infty} q(\xi) d\xi = \int_0^1 q(\xi) d\xi + \int_1^{\infty} [q(\xi) - q_*(\xi)] d\xi + \int_1^{\infty} q_*(\xi) d\xi$. Here the last integral can be evaluated in terms of special functions and the numerical evaluation of the second integral converges quickly due to the rapid decay of the integrand for large ξ . The numerical integrations were performed to six-digit accuracy.

The solution of the eigenvalue problem (3.67) determines a set of N eigenvalue pairs $(\lambda^{(m)}, \mathbf{u}^{(m)})$, $m = 1, \dots, N$. For each eigensolution (λ, \mathbf{u}) , we determine an island radius $\hat{R} = 1/2\lambda$, the coefficients in the Bessel series a_k from (3.68) and (3.48), the scale factor c from (3.69), and the chemical potential $\hat{\mu}$ from (3.74). This set of solutions for $m = 1, \dots, N$ correspond to N distinct island ‘modes.’

We calculate solutions corresponding to $N = 32$ terms, indexing the modes $m = 1, \dots, N$ by increasing radius \hat{R} . The eigenvalues and eigenvectors are all real. Figure 2 shows that the first four odd modes correspond to a center mound surrounded by $(m - 1)/2$ annular ridges. Figure 3 shows

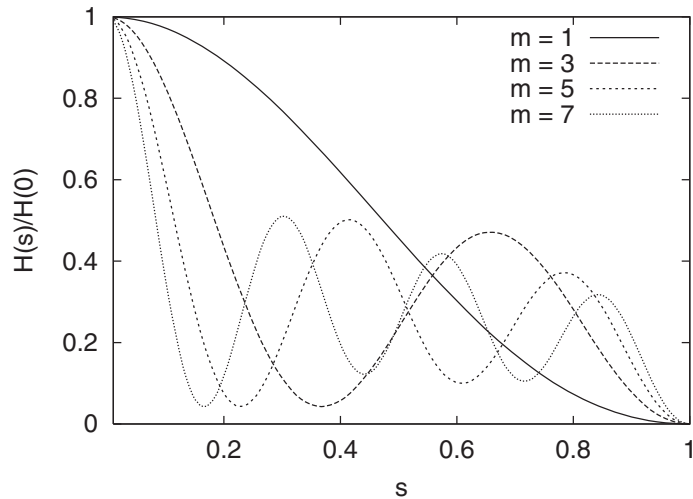


FIG. 2. Island shapes for odd modes $m = 1, 3, 5, 7$. Shown is the normalized island shape $H(s)/|H(0)|$.

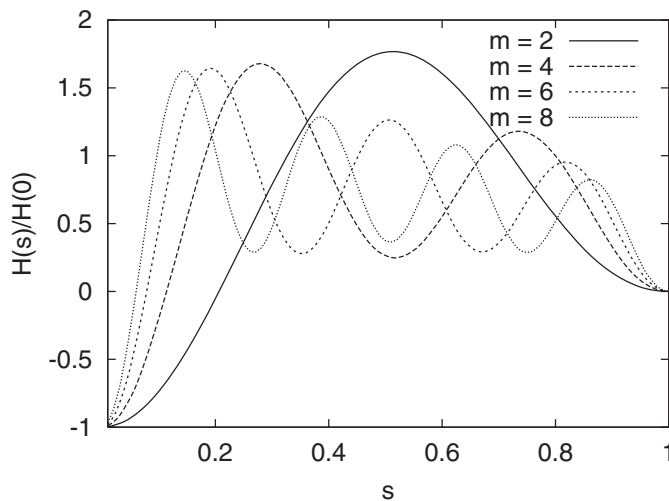


FIG. 3. Island shapes for even modes $m = 2, 4, 6, 8$. Shown is the normalized island shape $H(s)/|H(0)|$.

that the first four even modes correspond to a center pit surrounded by $m/2$ annular ridges. Note, however, that the even-mode solutions are not admissible solutions to the free boundary problem because the center pit extends into the substrate and violates the wetting constraint $H(s) \geq 0$. Results for larger m indicate that the pattern for the odd and even solutions continues. We conjecture (but offer no proof) that for $N = \infty$ all eigenvalues and eigenvectors are real, all odd modes have a center mound and $(m - 1)/2$ annular ridges, and all even modes have a center pit and $m/2$ annular ridges with the center pit in violation of the wetting constraint.

Table 1 gives the island radius and chemical potential for the modes $m = 1-8$. As m increases,

TABLE 1
Island radius and chemical potential for modes $m = 1-8$. Numerical values of $\hat{\mu}$ scale with v as $(1 + v)^3$ through the dependence of $\hat{\mu}$ on c (3.69). Results are for $v = 0.25$

m	\hat{R}	$\hat{\mu}$
1	2.061	-0.183 2
2	3.671	-0.039 23
3	5.259	-0.014 63
4	6.839	-0.007 028
5	8.416	-0.003 916
6	9.991	-0.002 406
7	11.565	-0.001 584
8	13.139	-0.001 098

TABLE 2
Convergence of solutions for the $m = 1$ and $m = 8$ modes

N	$m = 1$		$m = 8$	
	\hat{R}	$\hat{\mu}$	\hat{R}	$\hat{\mu}$
1	2.074 10	-0.182 224	-	-
2	2.065 11	-0.183 041	-	-
4	2.061 94	-0.183 159	-	-
8	2.060 96	-0.183 171	11.5962	-0.001 578 09
16	2.060 71	-0.183 171	13.1441	-0.001 098 19
32	2.060 66	-0.183 171	13.1387	-0.001 098 42

corresponding to an increasing number of ripples in the solution, the island radius increases as well. The chemical potential for these modes are all negative, with the $m = 1$ mode having the most negative $\hat{\mu}$. As m increases the chemical potential becomes less negative, apparently approaching zero as m increases.

Table 2 illustrates the fast convergence of the series expansions as a function of the number of terms in the expansion N , using the modes $m = 1$ and $m = 8$ as representative examples. We illustrate convergence of the series by monitoring two physically relevant quantities, the island width \hat{R} and the chemical potential $\hat{\mu}$. For the $m = 1$ mode, solutions with three-digit accuracy are obtained with $N = 4$. For the $m = 8$ mode, we note that for the $m = 8$ mode to exist we of course need to keep at least $N = 8$ terms. For $N = 16$ the $m = 8$ solutions are accurate to four digits.

The relative energies of the different morphological modes can be deduced from the chemical potential correction $\mu_1 = \hat{\mu}(1 + v)$. Note that since $\mu = 1 + \epsilon\mu_1 + \dots$, where $\epsilon = V$ is the island volume, a more negative μ_1 means a smaller chemical potential. In the dynamic problem, mass transport is through surface diffusion from regions of high chemical potential to regions of low chemical potential, so we infer the relative energetics of different modes from the chemical potential. Since μ_1 is negative, this means that all island modes are energetically preferred to a planar film ($\mu_1 = 0$). Since μ_1 is most negative for $m = 1$, this means that the $m = 1$ mode is energetically preferred for islands of fixed volume. Note also that since μ_1 is negative for all modes, the energy of all island modes decreases with increasing island volume.

Figure 4 shows the energetically preferred island shape corresponding to mode $m = 1$. Since

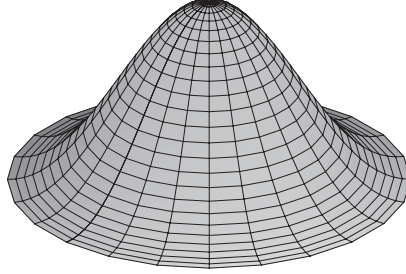


FIG. 4. 3D island corresponding to $m = 1$. Island height is normalized to unity.

our asymptotic theory is based on small island volume, our solutions describe islands for which the height is much smaller than the island width. To leading order the island width is fixed, and there is a direct scaling between the island volume and island height. Thus, as the volume increases from zero the island height increases proportionately but it retains a characteristic width and self-similar shape.

4. Discussion

4.1 Comparison with 2D island ridges

For the 2D island ridge described in [32], the fixed W value was 1.73, compared with the value of $4.122/(1 + \nu)$ for an axisymmetric island. Thus, for a typical value of $\nu = 0.25$, an axisymmetric island is wider than a 2D ridge by almost a factor of two. The difference in W for 2D and 3D axisymmetric islands is consistent with the difference in wavelengths for 2D and 3D neutrally stable sinusoidal perturbations. From the stability analysis of small-amplitude perturbations to a planar film of the form $e^{ia_x x + ia_y y}$, neutrally stable solutions are found to have [30]

$$a = \sqrt{a_x^2 + a_y^2} = 4. \quad (4.1)$$

A 2D perturbation is equivalent to $a_y = 0$, therefore $a_x = 4$. The corresponding wavelength is $\lambda = 2\pi/a_x = 1.57$. A 3D perturbation with equal wavelengths in x and y corresponds to $a_x = a_y = 4/\sqrt{2}$, with the wavelength in each direction $\lambda = 2\pi/a_x = 2\pi/a_y = 2.22$. Thus, the neutral 2D perturbation has a smaller wavelength than the neutral 3D perturbation, which is consistent with our observation that the equilibrium width of the 2D island ridge is smaller than the equilibrium width of an axisymmetric 3D island.

4.2 Comparison of first mode with experiment

To convert our solutions to dimensional (starred) coordinates we let $r^* = slR_0$ and $h^*(r^*) = H(s)l\epsilon R_0$, where $R_0 = \hat{R}/(1 + \nu)$, and $\epsilon = V^*/l^3$ is the scaled island volume. We compare our theoretical results with two studies of epitaxial growth of 3D islands, that by Eaglesham and Cerullo [7] for Ge islands on an Si substrate, and that by Albrecht *et al.* [1] for $\text{Ge}_{0.85}\text{Si}_{0.15}$ islands on an Si substrate. In order to compare the theoretical results with the experiments, we need the values of the relevant material parameters (elastic constants, lattice parameters, and surface energies). Using the anisotropic elastic constants for Ge and Si [16], we find isotropic values for the Lamé

TABLE 3

Material parameters used for interpolating composition-dependent material properties

Material	μ (10^{11} dynes cm^{-2})	λ (10^{11} dynes cm^{-2})	γ (erg cm^{-2})
Ge	5.64	3.76	1927
Si	6.81	5.24	2513

constants μ and λ by the Voigt averaging method [14]. Linear interpolation is used to approximate the corresponding constants for a $\text{Ge}_x\text{Si}_{1-x}$ alloy. The misfit strain $\epsilon_m = (a_S - a_F)/a_F$ is interpolated as $\epsilon_m(x) = x(a_{\text{Si}} - a_{\text{Ge}})/a_{\text{Ge}}$, where $a_{\text{Ge}} = 5.65754$ and $a_{\text{Si}} = 5.43072$ are the lattice parameters at room temperature [22]. The surface energy γ for pure Si and pure Ge is taken from [3]. We use linear interpolation to approximate $\gamma(x)$ for $\text{Ge}_x\text{Si}_{1-x}$ alloys (Table 3 shows the parameters for Ge and Si).

The length scale used to non-dimensionalize the elasticity problem was $l = \gamma/S_0$ where $S_0 = \frac{1}{2}T_{ij}E_{ij}$ is the basic-state strain energy, which for a biaxial misfit strain condition reduces to $S_0 = E\epsilon_m^2/(1 - \nu)$ where $E = \mu(2\mu + 3\lambda)/(\lambda + \mu)$ is Young's modulus and $\nu = \lambda/2(\lambda + \mu)$ is Poisson's ratio. Therefore the length scale as a function of the composition x is $l(x) = \gamma(x)[1 - \nu(x)]/E(x)(\epsilon_m(x))^2$. Using $W^* = 2R_0l(x)$ provides the expected island width as a function of film composition in dimensional units. Figure 5 illustrates the relationship between W^* and x for $\text{Ge}_x\text{Si}_{1-x}$ alloys on Si substrates. For a pure Ge layer on an Si substrate, the theoretical width W^* is 21.5 nm. Eaglesham and Cerullo [7] observed diameters of 40 nm for small isolated islands. For the $\text{Ge}_{0.85}\text{Si}_{0.15}$ layer on Si substrate $W^* = 30.2$ nm. Albrecht *et al.* [1] observed island base widths of approximately 50 nm. Thus, our theoretical results for W^* are within a factor of 2 of the experimentally observed island widths.

It is noted that the theoretical values for W^* are smaller than the corresponding experimental measurements. Factors which may contribute to this difference include:

- The difference in the elastic constants of the film and substrate: we assumed that the elastic constants of the film and substrate were the same. Table 3 shows, however, that the elastic shear moduli, μ , of Ge and Si differ by about 20%, where Si is stiffer. Spencer *et al.* [30] have shown that a stiff substrate increases the wavelength of steady-state perturbations to a planar film. Based on the correspondence between island widths and neutral perturbation wavelengths, this suggests that including the effect of the stiffer Si substrate would increase the predicted W^* values, bringing them closer to the experimental measurements.
- Higher-order effects: our results are based on an expansion in $\epsilon = V$, and are therefore valid in the limit of small islands. Calculations of the fully nonlinear shape for the 2D case [33] have shown that W increases as the island volume increases. We expect a similar trend to hold in the 3D case. Therefore, our asymptotic W^* results represent *minimum* island widths which are exceeded as the island increases in size. In this sense the theory is consistent with the experiments in that the predicted W^* values lie below the experimental values (which are for finite V).
- Anisotropic material properties: we assumed that the material properties were isotropic, which provides a tractable model. However, the experiments of Albrecht *et al.* [1] show that anisotropy in the properties leads to faceted island shapes and a dependence of the morphologies on the crystalline orientation of the substrate. The modification of our analysis to include anisotropic

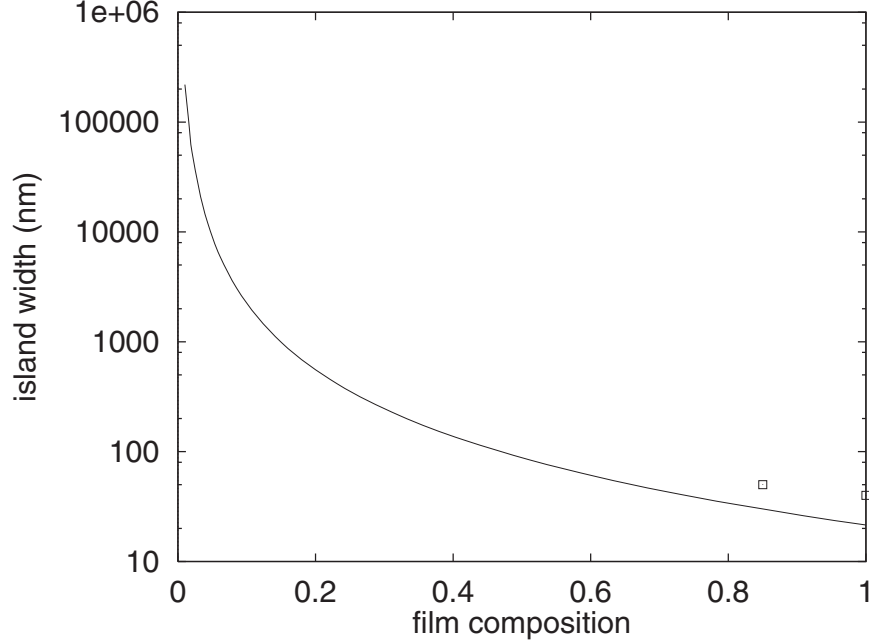


FIG. 5. Island width W^* versus film composition x for $\text{Ge}_x\text{Si}_{1-x}$ films on Si substrate. Data points are from observations discussed in the text.

material properties could result in changes to the predicted island widths and island shapes, particularly in the case of strong anisotropy.

4.3 *Quantum rings and quantum molecules*

The equilibrium solutions corresponding to modes $m > 1$ are not minimum energy configurations. Nonetheless, they may be metastable equilibrium states and may influence the evolution of the morphology in the fully dynamic problem. Morphologies such as ‘quantum rings’ and ‘quantum molecules’ observed in strained films [4] may be related to modes $m > 1$ in our theory. Figures 6 and 7 compare the observed quantum ring and quantum molecule morphologies in the CdTe/ZnTe system with our mode $m = 2$ and $m = 3$ solutions. There is a striking qualitative similarity.

We note that since our $m = 2$ mode violates the wetting constraint, it does not represent a true quantum ring morphology. To describe a quantum ring we must enforce the wetting constraint inside the ring, which would lead to a version of the axisymmetric problem where we would find annular solutions to the free boundary problem for which $h(r) > 0$ for $a < r < b$ with $h(r) = 0$ otherwise. For the quantum molecule solutions, close inspection of Fig. 7a shows that the ring structure is similar to our $m = 3$ mode but is modulated in the azimuthal direction. Such modulations can not be described within our axisymmetric theory, but there is the obvious generalization of our work to include an azimuthal dependence of the shape with trigonometric modes. It is possible that allowing for modulation in the azimuthal direction would lead to a lower energy solution than the axisymmetric mode (perhaps with a lowest energy solution having a circumferential modulation with wavelength similar to the width of the ring). Description of such a structure would require

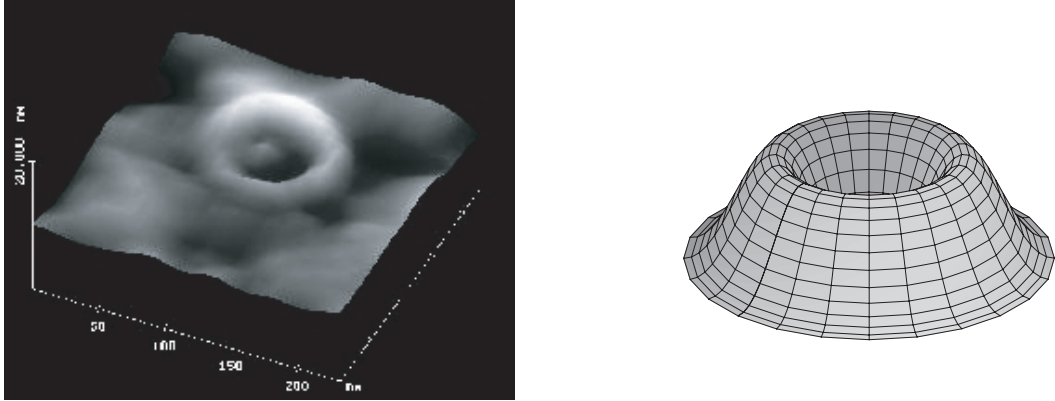


FIG. 6. Quantum ring morphologies. (a) Quantum ring observed in CdTe/ZnTe (courtesy of Luo), (b) mode $m = 2$ solution with height normalized to unity.

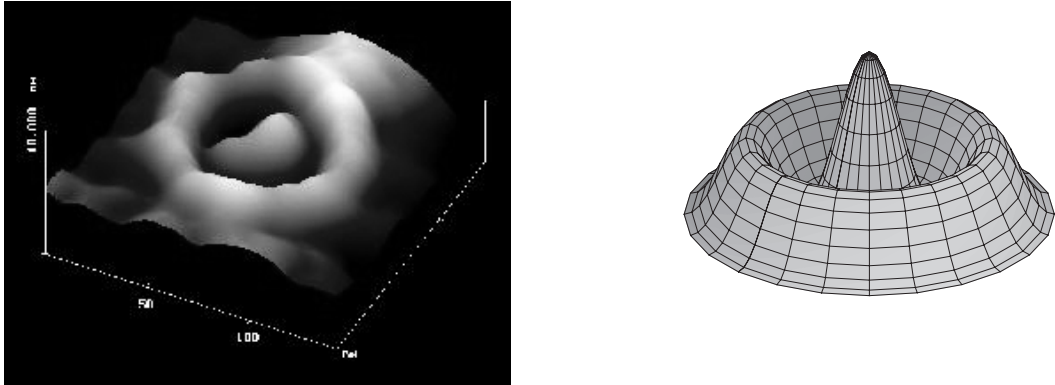


FIG. 7. Quantum molecule morphologies. (a) Quantum molecule observed in CdTe/ZnTe (courtesy of Luo), (b) mode $m = 3$ solution with height normalized to unity.

generalization of this work to describe a nonaxisymmetric morphology $h(r, \theta) > 0$ on $r < R(\theta)$, where now the curve that forms the island edge becomes a free boundary. Such generalizations might permit direct prediction of quantum ring and quantum molecule morphologies and their stability.

5. Summary

We have modeled the island morphology in strained solid films using a continuum theory with a glued wetting layer model for the film/substrate interactions. The resulting free boundary elasticity problem has a piecewise boundary equation for the island shape. We have found the shape of a small axisymmetric island by developing an asymptotic solution based on the island height being much smaller than the island width, which leads to a codimension-two free boundary problem. The use of a Hankel transform enabled us to determine the solution of the elasticity problem in terms of an island of arbitrary (thin) shape. Substitution of the general elasticity solution into the free boundary equation gave an integro-differential equation for the island shape in which the island

width played the role of an eigenvalue. We determined a rapidly converging solution to this integro-differential equation in terms of a Bessel series. We find a discrete spectrum of island widths and island modes. The first mode corresponds to a quantum dot and is the most energetically favorable mode. Our predictions of quantum dot width are within a factor of 2 of observations in SiGe/Si, and it is suggested that this discrepancy is due primarily to our assumption of equal elastic constants in the film and substrate, and to the nonlinear effect of the island size on the island width. Finally, the $m = 2$ and $m = 3$ modes are suggestive of quantum ring and quantum molecule morphologies. Generalizations of the present work to include (i) annular solutions and (ii) nonaxisymmetry might permit detailed description of the quantum ring and quantum molecule morphologies and their stability.

Acknowledgements

This research was supported by NSF grants DMS-9622930 and DMS-0072532 (B. J. S.). We thank C. M. Elliott for particularly helpful editorial comments.

REFERENCES

1. ALBRECHT, M., CHRISTIANSEN, S., MICHLER, J. *et al.* Surface ripples, crosshatch pattern, and dislocation formation—mechanisms in lattice mismatch relaxation. *Appl. Phys. Lett.* **67**, (1995) 1232–1234.
2. ASARO, R. J. & TILLER, W. A. Interface morphology development during stress corrosion cracking: part I. Via surface diffusion. *Metall. Trans.* **3**, (1972) 1789–1796.
3. BLAKELY, J. M. *Introduction to the Properties of Crystal Surfaces*. Pergamon, Oxford (1973).
4. CHEN, X., MOONEY, K. P., YEO, T., FURIS, M., LUO, H., MCCOMBE, B. D., & PETROU, A. Growth and characterization of digital alloys and heterostructures of GaAs/Mn. preprint: and Garcia, J. M., Medeiros-Ribeiro, O., Schmidt, K., Ngo, T., Feng, J. L., Lorke, A., Kotthaus, J. and Petroff, P. M. *Appl. Phys. Lett.* **71**, (1997) 2015–2017.
5. CHIU, C. H. & GAO, H. Stress singularities along a cycloid rough surface. *Int. J. Solids Struct.* **30**, (1993) 2983–3012.
6. CHIU, C. H. & GAO, H. A numerical study of stress controlled surface diffusion during epitaxial film growth. *Mater. Res. Soc. Symp. Proc.* **356**, (1995) 33–44.
7. EAGLESHAM, D. J. & CERULLO, M. Dislocation-free Stranski–Krastanow growth of Ge on Si(100). *Phys. Rev. Lett.* **64**, (1990) 1943–1946.
8. FREUND, L. B. & JONSDOTTIR, F. Instability of a biaxially stressed thin film on a substrate due to material diffusion over its free surface. *J. Mech. Phys. Solids* **41**, (1993) 1245–1264.
9. GAO, H. A boundary perturbation analysis for elastic inclusions and interfaces. *Int. J. Solids Struct.* **28**, (1991) 703–725.
10. GAO, H. Some general properties of stress-driven surface evolution in a heteroepitaxial thin film structure. *J. Mech. Phys. Solids* **42**, (1994) 741–772.
11. GRILHE, J. Study of roughness formation induced by homogeneous stress at the free surfaces of solids. *Acta Metall. Mater.* **41**, (1993) 909–913.
12. GRINFELD, M. A. Instability of the separation boundary between a non-hydrostatically stressed elastic body and a melt. *Sov. Phys. Dokl.* **31**, (1986) 831–834.
13. GRINFELD, M. A. The stress driven instability in elastic crystals: mathematical models and physical manifestations. *J. Nonlinear Sci.* **3**, (1993) 35–83.
14. HIRTH, J. P. *Theory of Dislocations*. Wiley-Interscience, New York (1982) pp. 430.
15. HOWISON, S. D., MORGAN, J. D., & OCKENDON, J. R. A class of codimension-two free boundary problems. *SIAM Rev.* **39**, (1997) 221–253.

16. HUNTINGTON, H. B. *The Elastic Constants of Crystals*. Academic, New York (1958) pp. 62.
17. JUNQUA, N. & GRILHÉ, J. Surface instabilities of epitaxial films on a substrate. *J. Phys. III France* **3**, (1993) 1589–1601.
18. KASSNER, K. & MISBAH, C. Non-linear evolution of a uniaxially stressed solid: a route to fracture? *Europhys. Lett.* **28**, (1994) 245–250.
19. KUKTA, R. V. & FREUND, L. B. Minimum energy configuration of epitaxial material clusters on a lattice-mismatched substrate. *J. Mech. Phys. Solids* **45**, (1997) 1835–1860.
20. LITTLE, R. W. *Elasticity*. Prentice-Hall, New York (1973) pp. 343–347.
21. LOVE, A. E. H. *A Treatise on the Mathematical Theory of Elasticity*. Dover, New York (1944).
22. LYNCH, C. T. *Handbook of Materials Science*. CRC Press, New York (1975) pp. 154.
23. PETROFF, P. M. & MEDEIROS-RIBEIRO, G. Three-dimensional carrier confinement in strain-induced self-assembled quantum dots. *MRS Bull.* **21**, (1996) 50–54.
24. POPOV, G. I. On a method of solution of the axisymmetric contact problem of the theory of elasticity. *J. Appl. Math. Mech.* **25**, (1961) 105–118.
25. SHCHUKIN, V. A. & BIMBERG, D. Spontaneous ordering of nanostructures on crystal surfaces. *Rev. Mod. Phys.* **71**, (1999) 1125–1171.
26. SNEDDON, I. N. *Fourier Transforms*. McGraw-Hill, New York (1951) pp. 58.
27. SPENCE, D. A. Self similar solutions to adhesive contact problems with incremental loading. *Proc. R. Soc. A* **305**, (1968a) 55–80.
28. SPENCE, D. A. A Wiener-Hopf equation arising in elastic contact problems. *Proc. R. Soc. A* **305**, (1968b) 81–92.
29. SPENCER, B. J., VOORHEES, P. W., & DAVIS, S. H. Morphological instability in epitaxially strained dislocation-free solid films. *Phys. Rev. Lett.* **67**, (1991) 3696–3699.
30. SPENCER, B. J., VOORHEES, P. W., & DAVIS, S. H. Morphological instability in epitaxially strained dislocation-free solid films: linear stability theory. *J. Appl. Phys.* **73**, (1993) 4955–4970.
31. SPENCER, B. J. & MEIRON, D. I. Nonlinear evolution of the stress-driven morphological instability in a two-dimensional semi-infinite solid. *Acta Metall. Mater.* **42**, (1994) 3629–3641.
32. SPENCER, B. J. & TERSOFF, J. Equilibrium shapes of small strained islands. *Mater. Res. Soc. Symp. Proc.* **399**, (1996) 283–288.
33. SPENCER, B. J. & TERSOFF, J. Equilibrium shapes and properties of epitaxially strained islands. *Phys. Rev. Lett.* **79**, (1997) 4858–4861.
34. SPENCER, B. J. & TERSOFF, J. Equilibrium shapes of islands in epitaxially strained solid films. In: GOLDEN, K. M., GRIMMETT, G. R., JAMES, R. D., MILTON, G. W. & SEN, P. N. (eds), *Mathematics of Multiscale Materials*. pp. 255–269. Springer, New York (1998).
35. SPENCER, B. J. An asymptotic derivation of the glued wetting layer model and contact angle condition for Stranski–Krastanow islands. *Phys. Rev. B* **59**, (1999) 2011–2017.
36. SROLOVITZ, D. J. On the stability of surfaces of stressed solids. *Acta Metall.* **37**, (1989) 621–625.
37. SROLOVITZ, D. J. & DAVIS, S. H. Do stresses modify wetting angles? *Acta Mater.* **49**, (2001) 1005–1007.
38. TERSOFF, J. Stress-induced layer-by-layer growth of Ge on Si(100). *Phys. Rev. B* **43**, (1991) 9377–9380.
39. YANG, W. H. & SROLOVITZ, D. J. Cracklike surface instabilities in stressed solids. *Phys. Rev. Lett.* **71**, (1993) 1593–1596.
40. YANG, W. H. & SROLOVITZ, D. J. Surface morphology evolution in stressed solids: surface diffusion controlled crack initiation. *J. Mech. Phys. Solids* **42**, (1994) 1551–1574.
41. ZHANG, Y. W. Formation of epitaxially strained islands during controlled annealing. *Appl. Phys. Lett.* **75**, (1999) 205–207.
42. ZHANG, Y. W. & BOWER, A. F. Numerical simulations of island formation in a coherent epitaxial thin film system. *J. Mech. Phys. Solids* **47**, (1999) 2273–2297.

Appendix.

Here we derive the elasticity solution to (3.20)–(3.24) for an arbitrary $h_0(r)$. The elasticity problem is a mixed boundary value problem for the half-space in which the applied shear stress vanishes outside of the island contact region. This mixed boundary value problem could be approached using the Wiener–Hopf method as has been done for axisymmetric elastic contact problems [24, 27, 28]. Here we choose to find the elasticity solution using Hankel transforms.

An axisymmetric stress function, $\phi(r, z)$ (Love’s stress function) [21], is introduced such that

$$\sigma_{rr} = \frac{\partial}{\partial z} \left(\nu \nabla^2 \phi - \frac{\partial^2 \phi}{\partial r^2} \right) \quad (\text{A.1})$$

$$\sigma_{\theta\theta} = \frac{\partial}{\partial z} \left(\nu \nabla^2 \phi - \frac{1}{r} \frac{\partial \phi}{\partial r} \right) \quad (\text{A.2})$$

$$\sigma_{zz} = \frac{\partial}{\partial z} \left[(2 - \nu) \nabla^2 \phi - \frac{\partial^2 \phi}{\partial z^2} \right] \quad (\text{A.3})$$

$$\tau_{rz} = \frac{\partial}{\partial r} \left[(1 - \nu) \nabla^2 \phi - \frac{\partial^2 \phi}{\partial z^2} \right], \quad (\text{A.4})$$

where we have dropped the superscript ‘1’ from the stresses. The stress function ϕ satisfies the mechanical equilibrium and compatibility conditions of linear elasticity if $\nabla^4 \phi = 0$. The stress depends on the shape $h_0(r)$ through the boundary condition (3.22). We use the Hankel transform [26] to relate the stresses to $h_0(r)$. The Hankel transform of order n of a function $f(r)$ is defined as

$$f^n(\xi) = H_n\{f(r); \xi\} = \int_0^\infty r f(r) J_n(\xi r) dr, \quad (\text{A.5})$$

where J_n is the Bessel function of order n . The inverse Hankel transform is then

$$f(r) = \int_0^\infty \xi f^n(\xi) J_n(\xi r) d\xi. \quad (\text{A.6})$$

We apply the Hankel transform of order zero to $\nabla^4 \phi = 0$ to obtain [20]

$$\left(\frac{\partial^2}{\partial z^2} - \xi^2 \right)^2 \int_0^\infty r \phi(r, z) J_0(\xi r) dr = 0. \quad (\text{A.7})$$

Letting $\phi^0(\xi, z) = \int_0^\infty r \phi(r, z) J_0(\xi r) dr$ gives the linear, fourth order, homogeneous differential equation

$$\frac{\partial^4 \phi^0}{\partial z^4} - 2\xi^2 \frac{\partial^2 \phi^0}{\partial z^2} + \xi^4 \phi^0 = 0. \quad (\text{A.8})$$

The general solution to (A.8) is $\phi^0(\xi, z) = (A + Bz\xi) e^{-\xi z} + (C + Dz\xi) e^{\xi z}$. For the solutions to decay as $z \rightarrow -\infty$, $A = B = 0$, and $\phi^0(\xi, z) = (C + Dz\xi) e^{\xi z}$. The constants C and D are determined by transforming the boundary conditions (3.22) and (3.23) for τ_{rz} and σ_{zz} . Using an

order-one Hankel transform for τ_{rz} and σ_{zz} in terms of ϕ provides [20]

$$H_1\{\tau_{rz}; \xi\} = (1 - \nu)\xi^3\phi^0 + \nu\xi\frac{\partial^2\phi^0}{\partial z^2} \quad (\text{A.9})$$

$$H_1\{\sigma_{zz}; \xi\} = (1 - \nu)\frac{\partial^3\phi^0}{\partial z^3} - (2 - \nu)\xi^2\frac{\partial\phi^0}{\partial z}. \quad (\text{A.10})$$

The transformed boundary conditions are then

$$H_1\{\tau_{rz}; \xi\} = g^1(\xi) \quad \text{on } z = 0 \quad (\text{A.11})$$

and

$$H_1\{\sigma_{zz}; \xi\} = 0 \quad \text{on } z = 0 \quad (\text{A.12})$$

where

$$g^1(\xi) = \int_0^\infty r \frac{dh_0}{dr} J_1(\xi r) dr \quad (\text{A.13})$$

is the order-one Hankel transform of dh_0/dr . Substituting for $\phi^0(\xi, z)$ in the transformed stress equations (A.9) and (A.10) and using the mechanical equilibrium boundary conditions (A.11) and (A.12), we determine C and D in terms of $g^1(\xi)$. The transformed Love function is therefore

$$\phi^0(\xi, z) = \frac{(1 - 2\nu + \xi z)e^{\xi z}}{\xi^3} g^1(\xi). \quad (\text{A.14})$$

The above elasticity solution (A.14) relates the stresses to the island shape. For a given $h_0(r)$, the function $g^1(\xi)$ is determined from the Hankel transform (A.13). Then, $\phi^0(\xi, z)$ is related to $g^1(\xi)$ from (A.14), and the stress function $\phi(r, z)$ is obtained by taking the inverse transform of $\phi^0(\xi, z)$.

For the free boundary equation (3.26) we need the strain energy density $S_1 = \sigma_{rr} + \sigma_{\theta\theta}$ on the surface of the film. A zero-order Hankel transform is used to express $(\sigma_{rr} + \sigma_{\theta\theta})$ in terms of ϕ^0 as

$$H_0\{\sigma_{rr} + \sigma_{\theta\theta}; \xi\} = (1 - 2\nu)\xi^2\frac{\partial\phi^0}{\partial z} + (2\nu)\frac{\partial^3\phi^0}{\partial z^3}. \quad (\text{A.15})$$

Substituting for $\phi^0(\xi, z)$ on $z = 0$ we obtain

$$H_0\{\sigma_{rr} + \sigma_{\theta\theta}; \xi\} = 2(1 + \nu)g^1(\xi). \quad (\text{A.16})$$

Substituting for $g^1(\xi)$ in the inverse transform of $H_0\{\sigma_{rr} + \sigma_{\theta\theta}; \xi\}$ gives the desired result

$$(\sigma_{rr} + \sigma_{\theta\theta}) = 2(1 + \nu) \int_0^\infty \xi \left[\int_0^\infty \hat{r} \frac{dh_0}{d\hat{r}} J_1(\xi \hat{r}) d\hat{r} \right] J_0(\xi r) d\xi. \quad (\text{A.17})$$